Appl. Phys. B 81, 235–244 (2005)
DOI: 10.1007/s00340-005-1877-3

Applied Physics B
Lasers and Optics

C.Y. KAO[1, ✉]
S. OSHER[2]
E. YABLONOVITCH[3]

Maximizing band gaps in two-dimensional photonic crystals by using level set methods

[1]Institute for Mathematics and its Applications (IMA), University of Minnesota, Minneapolis, MN 55455, USA
[2]Department of Mathematics, University of California Los Angeles, Los Angeles, CA 90095, USA
[3]Department of Electrical Engineering, University of California Los Angeles, Los Angeles, CA 90095, USA

Received: 1 February 2005 /
Revised version: 20 April 2005
Published online: 15 July 2005 • Springer-Verlag 2005

ABSTRACT The optimal design of photonic band gaps for two-dimensional square lattices is considered. We use the level set method to represent the interface between two materials with two different dielectric constants. The interface is moved by a generalized gradient ascent method. The biggest gap of GaAs in air that we found is 0.4418 for TM (transverse magnetic field) and 0.2104 for TE (transverse electric field).

PACS 42.70.Qs; 02.70.−c

1 Introduction

Photonic crystals are periodic dielectric structures which are designed to prevent the propagation of electromagnetic waves. They were first studied by Rayleigh in 1887 for one-dimensional layered structures. Later, Yablonovitch [1] and John [2] in 1987 introduced the concepts of photonic band gaps in two and three dimensions. Photonic crystals with band gaps have many applications. It is important to design an optimization algorithm to find photonic crystals with larger bandgaps. There have already been efforts [3–5] to solve such nano-photonic design problems by mathematical optimization. In Refs. [6] and [7], the authors proposed a projected generalized gradient ascent algorithm to maximize the band gaps iteratively for either transverse magnetic field or transverse electric field in two-dimensional photonic crystals. The optimized structure prefers a piecewise-constant dielectric distribution. Based on this, we resort to level set methods [8] to represent the interface between two materials with different dielectric constants. The front is moved by a generalized gradient ascent method. We test our algorithm for maximizing band gaps for either transverse magnetic field or transverse electric field in two-dimensional photonic crystals.

2 Governing equations

Suppose that there is no current or electric charge and the electromagnetic waves are monochromatic, i.e. $E(x,t) = E(x)\mathrm{e}^{-\mathrm{i}\omega t}$ and $H(x,t) = H(x)\mathrm{e}^{-\mathrm{i}\omega t}$. Maxwell's equations can be reduced to the following system:

$$\frac{1}{\epsilon(x)}\nabla \times (\nabla \times E(x)) = \frac{\omega^2}{c^2}E(x), \tag{1}$$

$$\nabla \times \frac{1}{\epsilon(x)}(\nabla \times H(x)) = \frac{\omega^2}{c^2}H(x), \tag{2}$$

where ϵ is the dielectric function. Suppose that the medium is isotropic, the magnetic permeability is constant, and the dielectric function is periodic, i.e. $\epsilon(x + R_\mathrm{i}) = \epsilon(x)$ for some primitive lattice vectors R_i. In TM[1] (transverse magnetic field), the magnetic field is in the $x\,y$ plane and the electric field $E = (0, 0, E)$ is perpendicular to the z axis. In TE (transverse electric field), the electric field is in the $x\,y$ plane and the magnetic field $H = (0, 0, H)$ is perpendicular to the z axis. Thus, the equations become

$$-\frac{1}{\epsilon(x)}\nabla \cdot (\nabla E(x)) = \frac{\omega^2}{c^2}E(x), \tag{3}$$

$$-\nabla \cdot \left(\frac{1}{\epsilon(x)}\nabla H(x)\right) = \frac{\omega^2}{c^2}H(x). \tag{4}$$

Applying Bloch's theorem, the solution can be characterized as follows: $E = \mathrm{e}^{\mathrm{i}\alpha\cdot x}E_\alpha$ and $H = \mathrm{e}^{\mathrm{i}\alpha\cdot x}H_\alpha$ with $E_\alpha(x + R_\mathrm{i}) = E_\alpha(x)$ and $H_\alpha(x + R_\mathrm{i}) = H_\alpha(x)$, where α is a wave number in the first Brillouin zone. E_α and H_α satisfy

$$-\frac{1}{\epsilon(x)}(\nabla + \mathrm{i}\alpha)\cdot(\nabla + \mathrm{i}\alpha)E_\alpha = \frac{\omega_{\mathrm{TM}}^2}{c^2}E_\alpha, \tag{5}$$

$$-(\nabla + \mathrm{i}\alpha)\cdot\frac{1}{\epsilon(x)}(\nabla + \mathrm{i}\alpha)H_\alpha = \frac{\omega_{\mathrm{TE}}^2}{c^2}H_\alpha, \tag{6}$$

with eigenvalues $\lambda_{\mathrm{TM}} = \omega_{\mathrm{TM}}^2/c^2$ and $\lambda_{\mathrm{TE}} = \omega_{\mathrm{TE}}^2/c^2$. Furthermore, if photonic crystals possess additional symmetries, we can consider solutions only in the irreducible Brillouin zone. There are several methods [10–12] designed to solve Eqs. (5) and (6) for given $\epsilon(x)$ and α. Here we use a finite-difference method to discretize Eqs. (5) and (6). After discretization, an eigenvalue problem is obtained. In Refs. [14, 15], inverse iteration together with multigrid acceleration is used to solve it efficiently. In our implementation, we simply use the Matlab routine eigs.

✉ Fax: +1-612-626-7370, E-mail: kao@ima.umn.edu

[1]We are following the convention from Joannopoulos' book [9], opposite to the usual meaning of TE and TM, as understood to be the field transverse to the wave vector **k**.

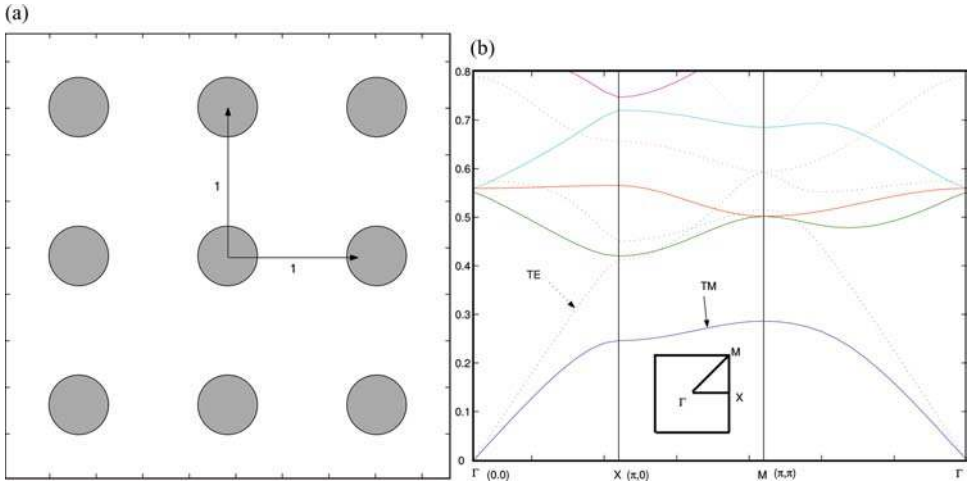

FIGURE 1 A 3 × 3 array of unit lattice (a. left) and its band structure (b. right)

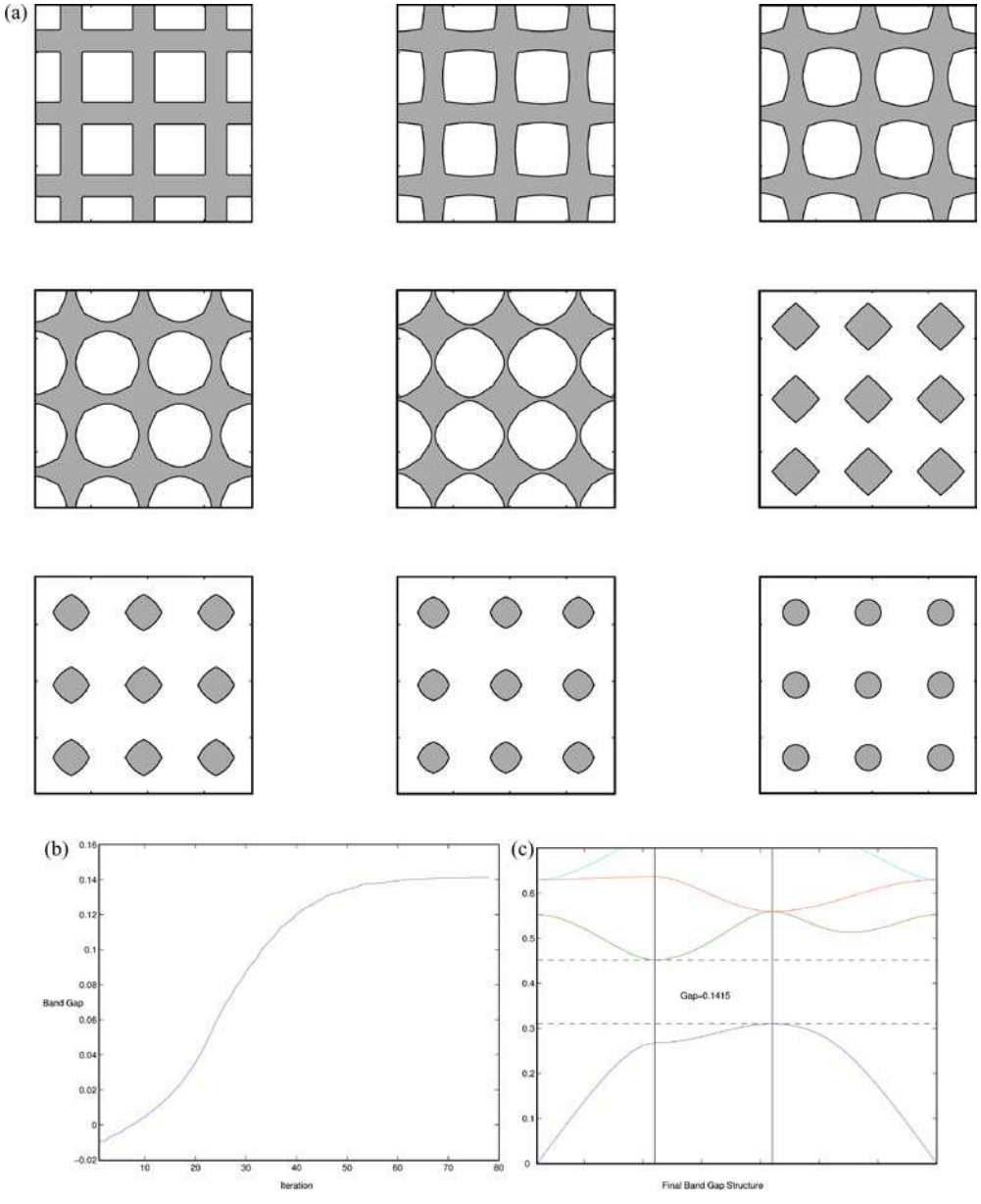

FIGURE 2 **a** The evolution of the dielectric distribution (top) **b** The band gap vs the iteration (bottom left) **c** The final band structure for maximizing the band gap between ω^1_{TM} and ω^2_{TM} (bottom right)

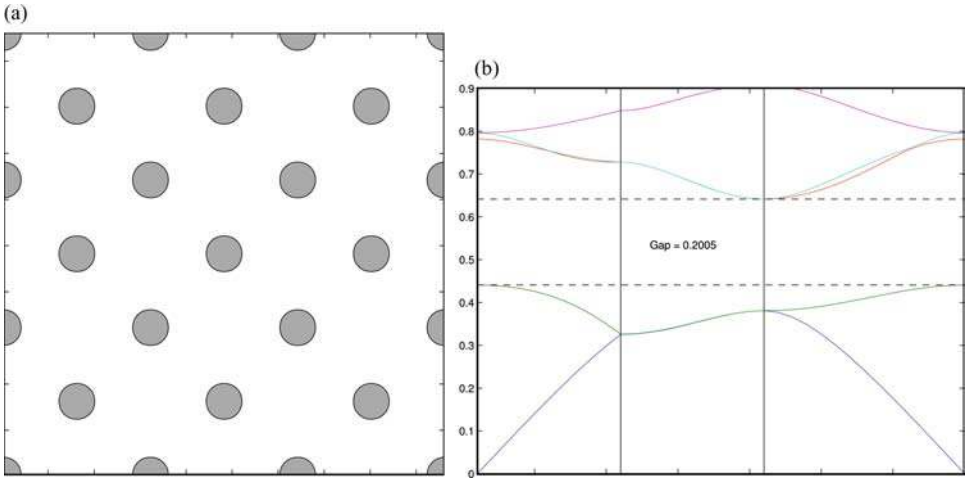

FIGURE 3 The dielectric distribution (a. left) and band structure (b. right) for maximizing the band gap between ω^2_{TM} and ω^3_{TM}

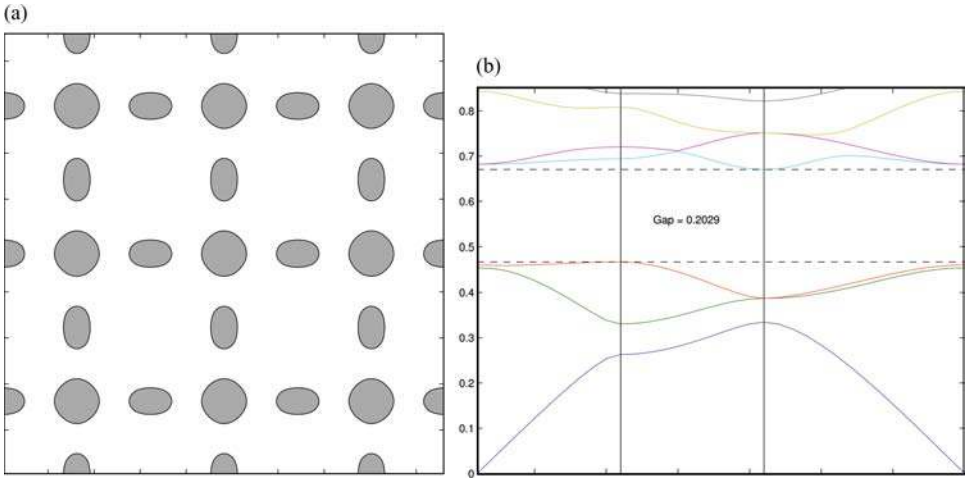

FIGURE 4 The dielectric distribution (a. left) and band structure (b. right) for maximizing the band gap between ω^3_{TM} and ω^4_{TM}

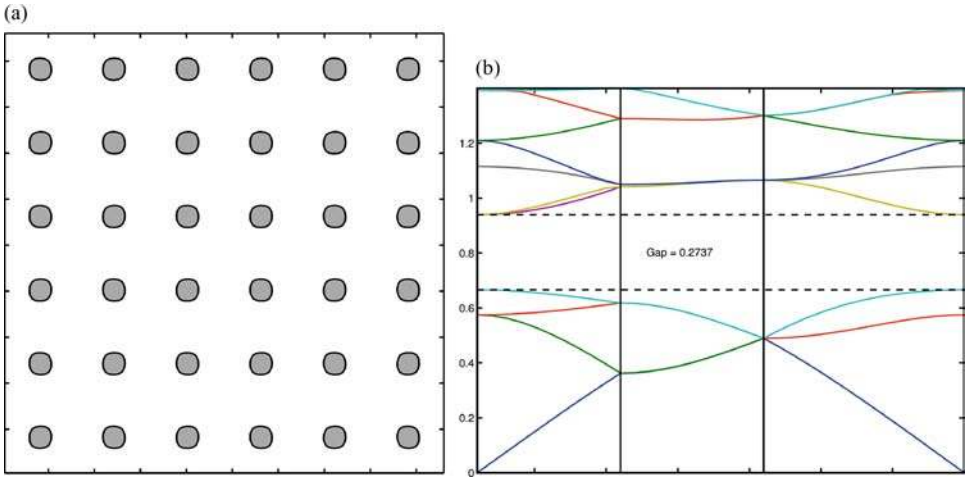

FIGURE 5 The dielectric distribution (a. left) and band structure (b. right) for maximizing the band gap between ω^4_{TM} and ω^5_{TM}

3 Level set formulation and gradient approach

We use the level set method [8, 16] to represent the interface between two materials with two different dielectric constants. Let

$$\epsilon = \begin{cases} \epsilon_1 & \text{for } \{x : \phi(x) < 0\}, \\ \epsilon_2 & \text{for } \{x : \phi(x) > 0\}. \end{cases}$$

The level set function is updated by solving the Hamilton–Jacobi equation

$$\phi_t + V\,|\nabla\phi| = 0, \tag{7}$$

where the velocity V gives the correct direction to optimize the desired design. Without loss of generality, we can choose $c = 1$. The optimization problems we solve here are

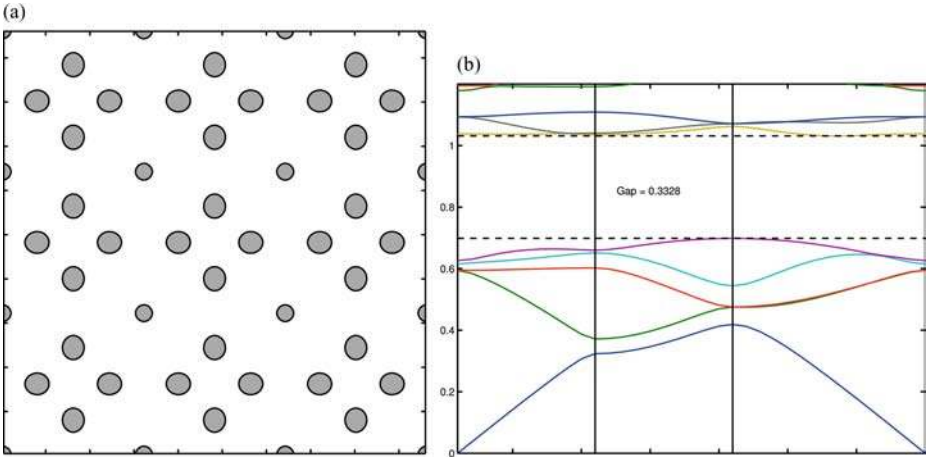

FIGURE 6 The dielectric distribution (a. left) and band structure (b. right) for maximizing the band gap between ω_{TM}^{5} and ω_{TM}^{6}

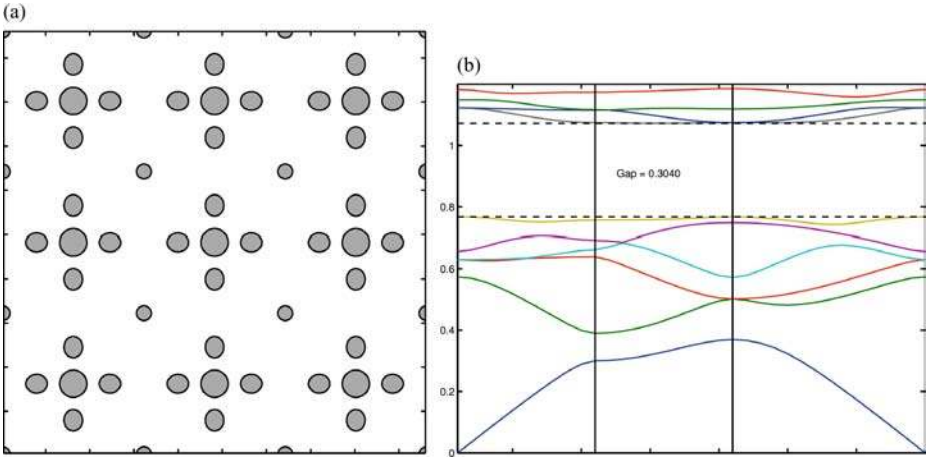

FIGURE 7 The dielectric distribution (a. left) and band structure (b. right) for maximizing the band gap between ω_{TM}^{6} and ω_{TM}^{7}

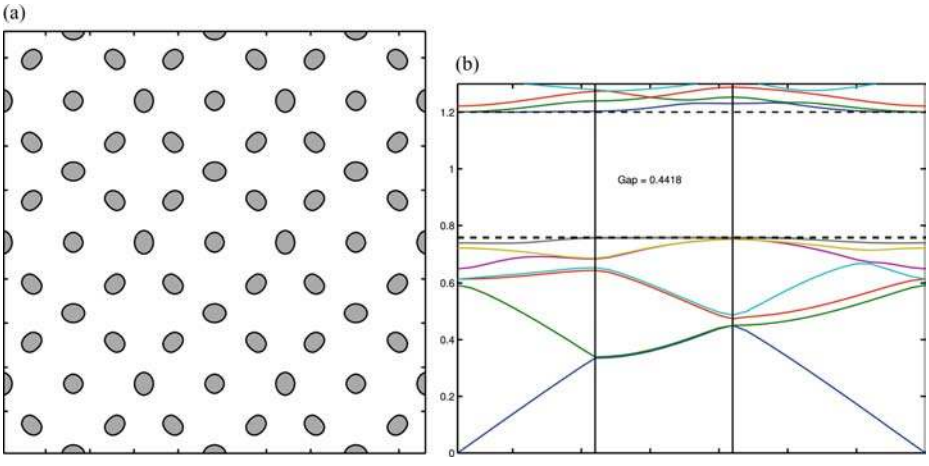

FIGURE 8 The dielectric distribution (a. left) and band structure (b. right) for maximizing the band gap between ω_{TM}^{7} and ω_{TM}^{8}

1. Maximize the band gap in TM:

$$\sup_{\phi}\left(\inf_{\alpha}\omega_{\mathrm{TM}}^{\mathrm{n}+1}-\sup_{\alpha}\omega_{\mathrm{TM}}^{\mathrm{n}}\right).$$

2. Maximize the band gap in TE:

$$\sup_{\phi}\left(\inf_{\alpha}\omega_{\mathrm{TE}}^{\mathrm{m}+1}-\sup_{\alpha}\omega_{\mathrm{TE}}^{\mathrm{m}}\right).$$

We denote the convex hull by co. The generalized gradients [6, 7, 17] with respect to ϕ can be written as follows:

$$\partial_{\phi}\omega_{\mathrm{TM}}^{\mathrm{k}}\subset co\left\{-\frac{1}{2}\left(\epsilon_2-\epsilon_1\right)\omega_{\mathrm{TM}}^{\mathrm{k}}|u|^2:\ u\in\Upsilon_{\mathrm{TM}}^{\mathrm{k}}(\epsilon,\alpha)\right\},\quad(8)$$

$$\partial_{\phi}\omega_{\mathrm{TE}}^{\mathrm{k}}\subset co\left\{\frac{1}{2\omega_{\mathrm{TE}}^{\mathrm{k}}}\left(\frac{1}{\epsilon_2}-\frac{1}{\epsilon_1}\right)\times|(\nabla+\mathrm{i}\alpha)v|^2:v\in\Upsilon_{\mathrm{TE}}^{\mathrm{k}}(\epsilon,\alpha)\right\},\quad(9)$$

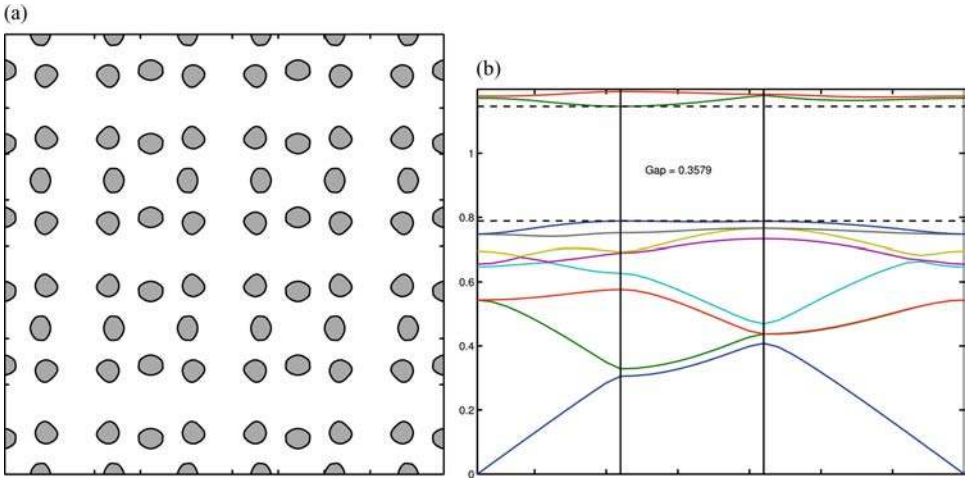

FIGURE 9 The dielectric distribution (a. left) and band structure (b. right) for maximizing the band gap between ω^8_{TM} and ω^9_{TM}

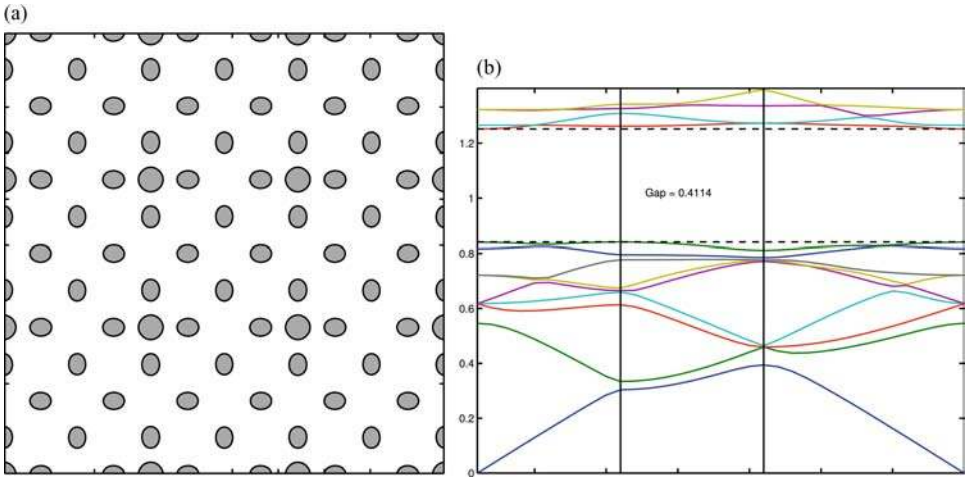

FIGURE 10 The dielectric distribution (a. left) and band structure (b. right) for maximizing the band gap between ω^9_{TM} and $\omega^{10}_{\mathrm{TM}}$

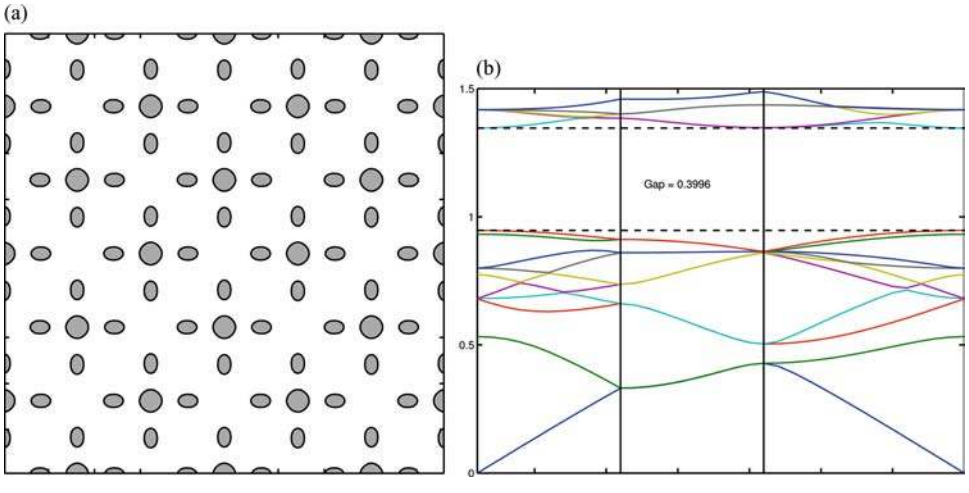

FIGURE 11 The dielectric distribution (a. left) and band structure (b. right) for maximizing the band gap between $\omega^{10}_{\mathrm{TM}}$ and $\omega^{11}_{\mathrm{TM}}$

where $\Upsilon^{\mathrm{k}}_{\mathrm{TM}}$ (and $\Upsilon^{\mathrm{k}}_{\mathrm{TE}}$) are the span of all eigenfunctions u (and v) associated with the eigenvalues $\lambda^{\mathrm{k}}_{\mathrm{TM}}$ (and $\lambda^{\mathrm{k}}_{\mathrm{TE}}$), respectively, and satisfying the normalization $\int_\Omega \epsilon|u|^2 = 1$ and $\int_\Omega |v|^2 = 1$. The corresponding velocities which give the ascent direction for the optimization are

1. $$V_{\mathrm{TM}} = co\left\{-\frac{1}{2}(\epsilon_2-\epsilon_1)\,\omega^{\mathrm{n+1}}_{\mathrm{TM}}|u|^2 : u \in \Upsilon^{\mathrm{n+1}}_{\mathrm{TM}}(\epsilon,\alpha)\right\} - co\left\{-\frac{1}{2}(\epsilon_2-\epsilon_1)\,\omega^{\mathrm{n}}_{\mathrm{TM}}|u|^2 : u \in \Upsilon^{\mathrm{n}}_{\mathrm{TM}}(\epsilon,\alpha)\right\}.$$

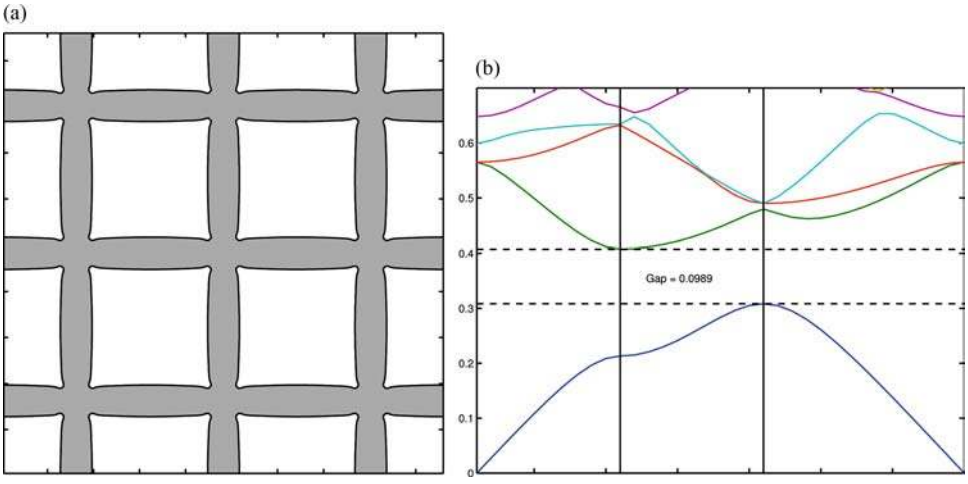

FIGURE 12 The dielectric distribution (a. left) and band structure (b. right) for maximizing the band gap between ω_{TE}^{1} and ω_{TE}^{2}

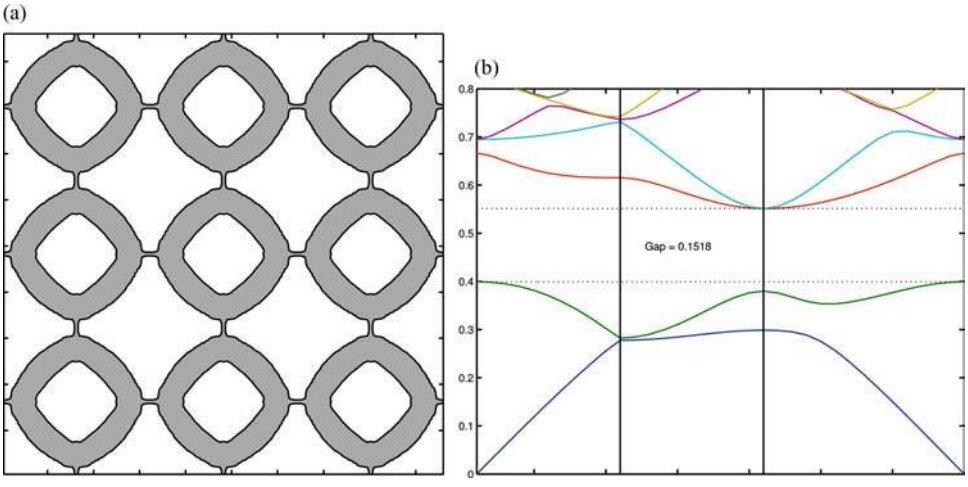

FIGURE 13 The dielectric distribution (a. left) and band structure (b. right) for maximizing the band gap between ω_{TE}^{2} and ω_{TE}^{3}

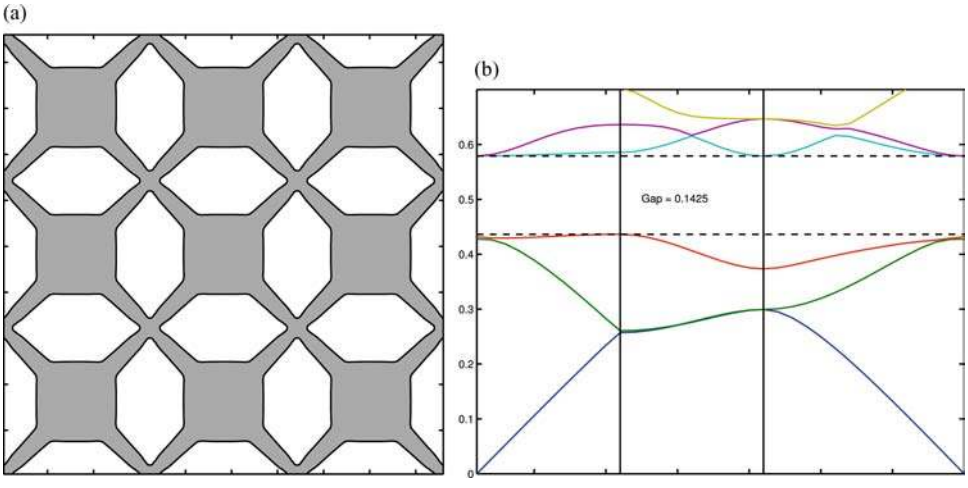

FIGURE 14 The dielectric distribution (a. left) and band structure (b. right) for maximizing the band gap between ω_{TE}^{3} and ω_{TE}^{4}

2. $V_{\mathrm{TE}} = co\left\{\frac{1}{2\omega_{\mathrm{TE}}^{\mathrm{m+1}}}\left(\frac{1}{\epsilon_2}-\frac{1}{\epsilon_1}\right)|(\nabla+\mathrm{i}\alpha)v|^2 : v \in \Upsilon_{\mathrm{TE}}^{\mathrm{m+1}}(\epsilon,\alpha)\right\}$

$$- co\left\{\frac{1}{2\omega_{\mathrm{TE}}^{\mathrm{m}}}\left(\frac{1}{\epsilon_2}-\frac{1}{\epsilon_1}\right)|(\nabla+\mathrm{i}\alpha)v|^2 : v \in \Upsilon_{\mathrm{TE}}^{\mathrm{m}}(\epsilon,\alpha)\right\}.$$

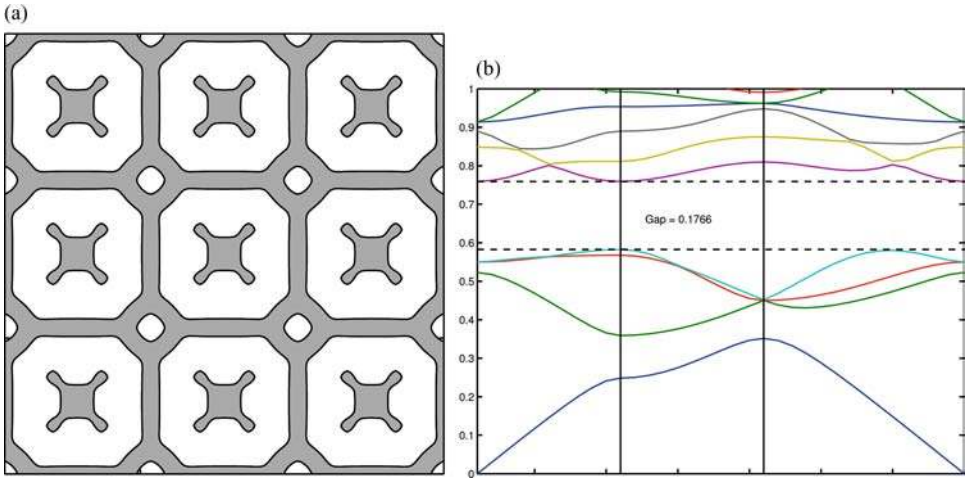

FIGURE 15 The dielectric distribution (a. left) and band structure (b. right) for maximizing the band gap between ω_{TE}^4 and ω_{TE}^5

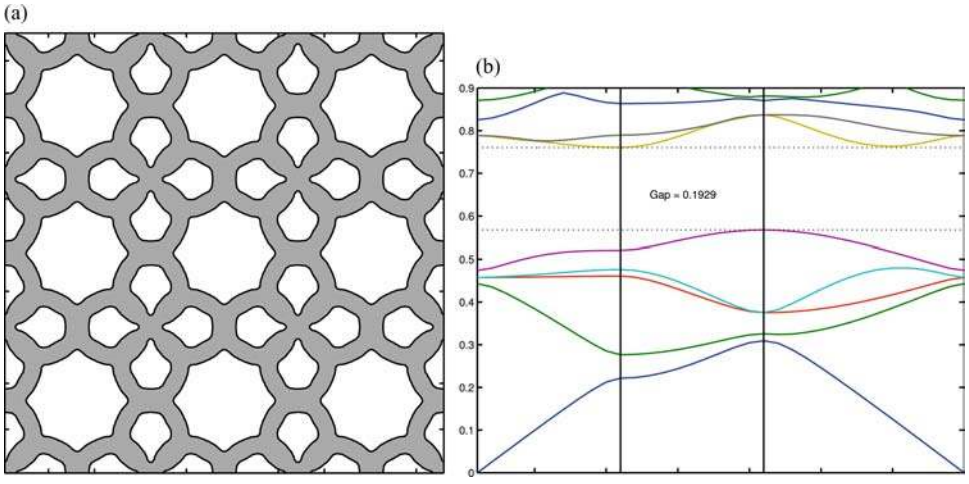

FIGURE 16 The dielectric distribution (a. left) and band structure (b. right) for maximizing the band gap between ω_{TE}^5 and ω_{TE}^6

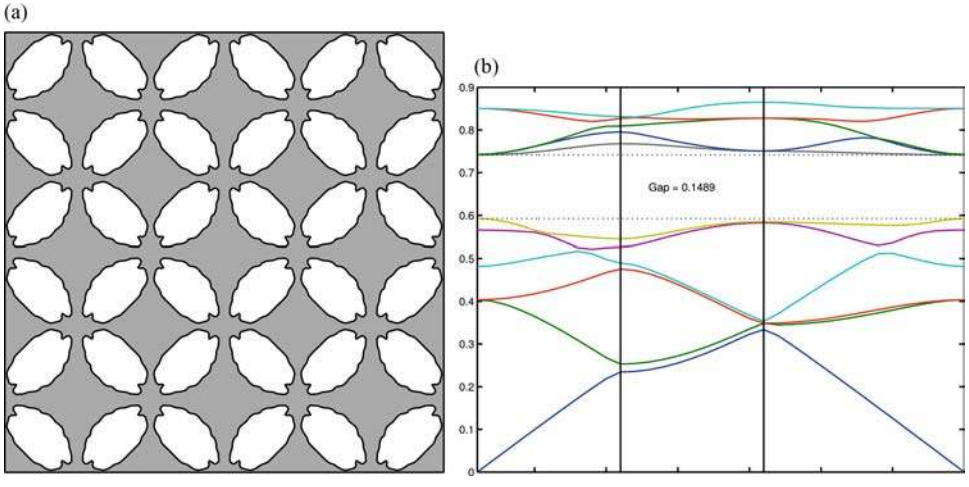

FIGURE 17 The dielectric distribution (a. left) and band structure (b. right) for maximizing the band gap between ω_{TE}^6 and ω_{TE}^7

Sometimes the band-gap ratio is also interesting. This can be optimized easily by using the chain rule to obtain the generalized ascent directions.

The basic algorithm can be summarized as follows:

1. First choose the initial ϵ and decide which band gap we want to maximize.
2. For $i = 0, 1, 2, \ldots$, find the velocity V which gives an ascent direction and a step size t_i to yield an increase in the objective band gap. Use the level set method (Eq. ((7)) to update ϕ and then obtain the new ϵ.

4 Results and conclusions

To implement the algorithm above, we choose the relative permittivity $\epsilon = \epsilon_2/\epsilon_1 = 11.4$, which is the case for GaAs in air. We consider a photonic crystal which is made

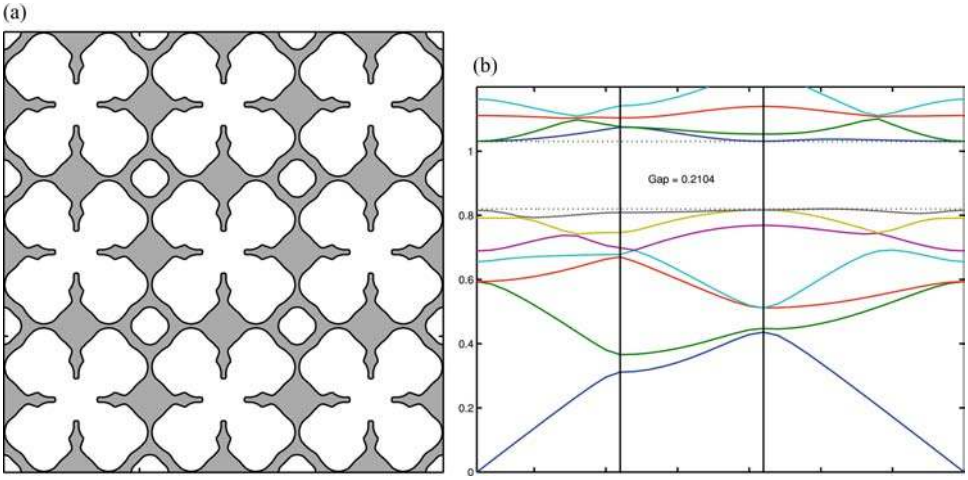

FIGURE 18 The dielectric distribution (a. left) and band structure (b. right) for maximizing the band gap between ω_{TE}^{7} and ω_{TE}^{8}

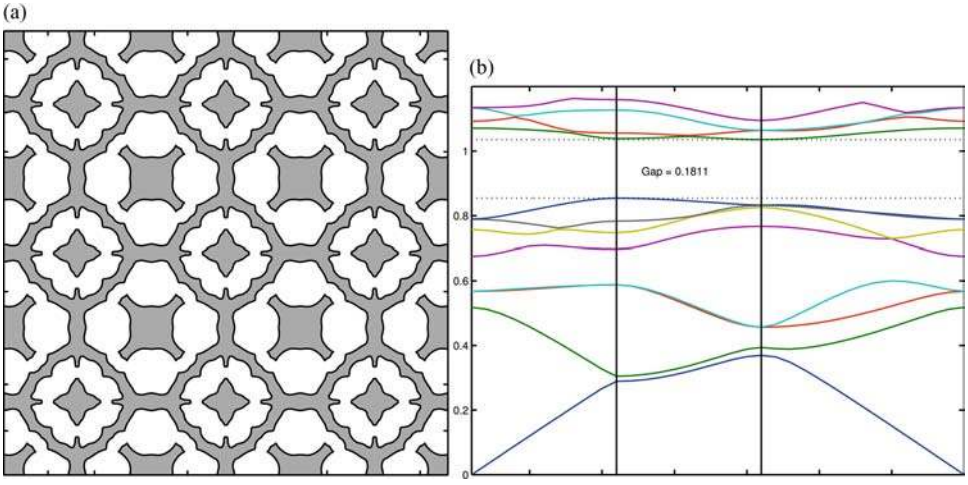

FIGURE 19 The dielectric distribution (a. left) and band structure (b. right) for maximizing the band gap between ω_{TE}^{8} and ω_{TE}^{9}

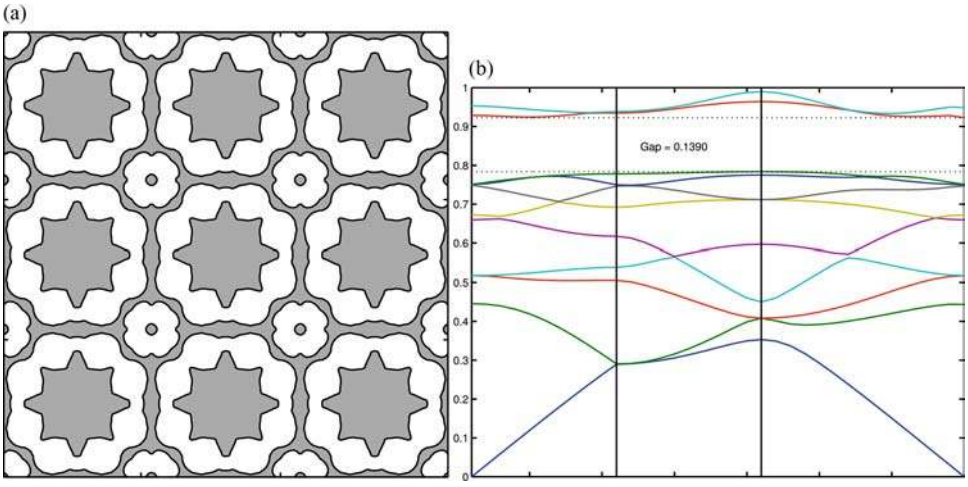

FIGURE 20 The dielectric distribution (a. left) and band structure (b. right) for maximizing the band gap between ω_{TE}^{9} and $\omega_{\mathrm{TE}}^{10}$

using a square lattice and has rotation, mirror-reflection, and inversion symmetry. In all numerical simulations, the computational domain is a unit square domain $\Omega = [-0.5\,,\ 0.5] \times [-0.5\,,\ 0.5]$ and the mesh sizes are $\frac{1}{64}$ (64 by 64 grid). Figure 1 shows a photonic crystal with square lattice and the corresponding band structure in the irreducible Brillouin zone of the reciprocal lattice. A 3×3 array of the unit lattice is shown for clarity. The light color indicates the low dielectric constant $\epsilon = 1$ while the dark color indicates the high dielectric constant $\epsilon = 11.4$.

In Fig. 2, we demonstrate the process of optimizing the band gap for the first and second eigenvalues in TM. As the

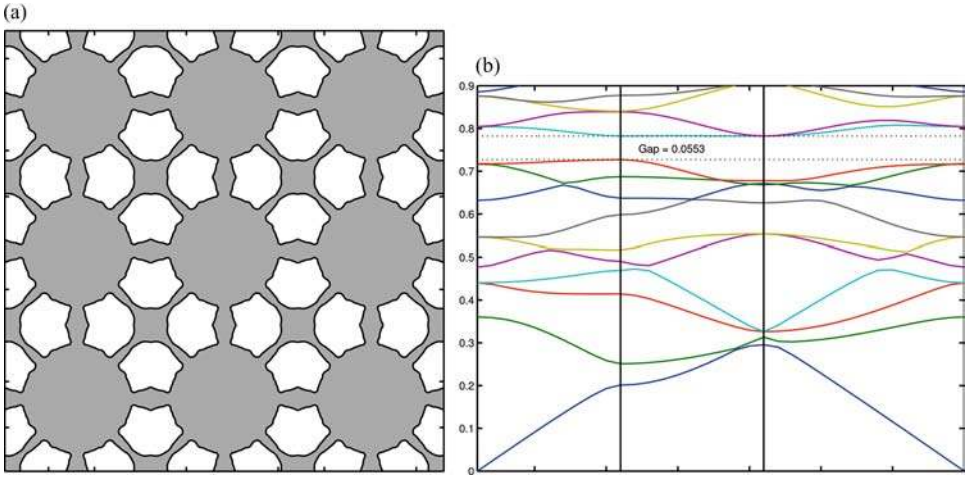

FIGURE 21 The dielectric distribution (a. left) and band structure (b. right) for maximizing the band gap between $\omega_{\mathrm{TE}}^{10}$ and $\omega_{\mathrm{TE}}^{11}$

number of iterations increases, the band gap gradually increases until it reaches a stable value, see Fig. 2b. The high ϵ region breaks and becomes circle finally as shown in Fig. 2a. Figure 2c shows the final optimized band structure. The topological change of dielectric distribution is well captured with the level set method.

For Figs. 3–21, we only plot the final optimized structure for the band gap between different adjacent frequencies. The results show that a lattice of isolated high ϵ region is preferred in TM while a lattice of connected high ϵ region is preferred in TE. The optimized structures may be invariant to rotation and rescaling, as shown in Figs. 2a and 3a. For structures with band gaps between higher adjacent frequencies in TM, composite geometries are presented in Figs. 6–8 and 10. The structures become even more complicated in TE; for example, see Figs. 18–21. Without numerical simulations, it would be very difficult to create such structures using physical intuition. We also observed that the gap in TM is usually easy to find and optimize. In TE, the objective function is 'more' nonconvex. The optimized results we found are probably only local maxima. The biggest gap we found is 0.4418 in TM and 0.2104 in TE. To the best of our knowledge, these give the largest band gaps that have been reported for a two-dimensional square lattice so far.

In the future, we will also apply the method to maximize the full band gap [18, 19] for both transverse magnetic field and transverse electric field:

$$\sup_{\phi}\left(\inf\left(\inf_{\alpha}\omega_{\mathrm{TM}}^{\mathrm{n+1}},\inf_{\alpha}\omega_{\mathrm{TE}}^{\mathrm{m+1}}\right)-\sup\left(\sup_{\alpha}\omega_{\mathrm{TM}}^{\mathrm{n}},\sup_{\alpha}\omega_{\mathrm{TE}}^{\mathrm{m}}\right)\right) \tag{10}$$

The velocity can be derived as

$$V_{\mathrm{EH}}=co\left\{co\left\{-\frac{1}{2}(\epsilon_2-\epsilon_1)\omega_{\mathrm{TM}}^{\mathrm{n+1}}|u|^2:\right.\right.$$
$$\left.\left.u\in\Upsilon_{\mathrm{TM}}^{\mathrm{n+1}}(\epsilon,\alpha)\right\},\right.$$
$$co\left\{\frac{1}{2\omega_{\mathrm{TE}}^{\mathrm{m+1}}}\left(\frac{1}{\epsilon_2}-\frac{1}{\epsilon_1}\right)|(\nabla+\mathrm{i}\alpha)v|^2:\right.$$
$$\left.v\in\Upsilon_{\mathrm{TE}}^{\mathrm{m+1}}(\epsilon,\alpha)\right\}:$$
$$\left.\alpha\in\operatorname{argmin}\left(\inf_{\alpha}\omega_{\mathrm{TM}}^{\mathrm{n+1}},\inf_{\alpha}\omega_{\mathrm{TE}}^{\mathrm{m+1}}\right)\right\}$$
$$co\left\{co\left\{-\frac{1}{2}(\epsilon_2-\epsilon_1)\omega_{\mathrm{TM}}^{\mathrm{n+1}}|u|^2:u\in\Upsilon_{\mathrm{TM}}^{\mathrm{n+1}}(\epsilon,\alpha)\right\},\right.$$
$$co\left\{\frac{1}{2\omega_{\mathrm{TE}}^{\mathrm{m+1}}}\left(\frac{1}{\epsilon_2}-\frac{1}{\epsilon_1}\right)|(\nabla+\mathrm{i}\alpha)v|^2:\right.$$
$$\left.v\in\Upsilon_{\mathrm{TE}}^{\mathrm{m+1}}(\epsilon,\alpha)\right\}:$$
$$\left.\alpha\in\operatorname{argmin}\left(\sup_{\alpha}\omega_{\mathrm{TM}}^{\mathrm{n}},\sup_{\alpha}\omega_{\mathrm{TE}}^{\mathrm{m}}\right)\right\}.$$

The results will be reported in another paper.

ACKNOWLEDGEMENTS The authors would like to thank M. Burger, Chien-C. Chang, C.-Chung Chang, R.L. Chern, and J.R. McLaughlin for useful discussions. This research was supported by NSEC Grant No. NSF DMI 0327077.

REFERENCES

1 E. Yablonovitch, Phys. Rev. Lett. **58**, 2059 (1987)
2 S. John, Phys. Rev. Lett. **58**, 2486 (1987)
3 J.M. Geremia, J. Williams, H. Mabuchi, Phys. Rev. E **66**, 66606 (2002)
4 Y. Chen, R. Yu, W. Li, O. Nohadani, S. Haas, A.F.J. Levi, J. Appl. Phys. **94**, 6065 (2003)
5 J.S. Jensen, O. Sigmund, J. Opt. Soc. Am. B **22**, 1191 (2005)
6 S.J. Cox, D.C. Dobson, SIAM J. Appl. Math. **59**, 2108 (1999)
7 S.J. Cox, D.C. Dobson, J. Comput. Phys. **158**, 214 (2000)
8 S. Osher, J.A. Sethian, J. Comput. Phys. **79**, 12 (1988)
9 J. Joannopoulos, R.D. Meade, J. Winn, Photonic Crystal Princeton, Princeton, NJ (1995)

10 K.M. Ho, C.T. Chan, C.M. Soukoulis, Phys. Rev. Lett. **65**, 3152 (1990)
11 Z. Zhang, S. Satpathy, Phys. Rev. Lett. **65**, 2650 (1990)
12 D. Dobson, J. Comput. Phys. **149**, 363 (1999)
13 D. Dobson, J. Gopalakrishnan, J.E. Pasciak, J. Comput. Phys. **161**, 668 (2000)
14 D. Hermann, M. Frank, K. Busch, P. Wolfle, Opt. Express **8**, 167 (2001)
15 R.L. Chern, C. Chung Chang, Chien C. Chang, R.R. Hwang, Phys. Rev. E **68**, 026704 (2003)
16 S.J. Osher, F. Santosa, J. Comput. Phys. **171**, 272 (2001)
17 S.J. Cox, J. Funct. Anal. **133**, 30 (1995)
18 M. Qiu, S. He, J. Opt. Soc. Am. B **17**, 1027 (2000)
19 L. Shen, Z. Ye, S. He, Phys. Rev. B **68**, 035109 (2003)